Biosensors and Bioelectronics 213 (2022) 114477

Contents lists available at ScienceDirect

Biosensors and Bioelectronics

journal homepage: www.elsevier.com/locate/bios

Bicyclic peptide-based assay for uPA cancer biomarker

Giulia Moro [a,1], Patrick Severin Sfragano [b,1], Jessica Ghirardo [a], Ylenia Mazzocato [a], Alessandro Angelini [a,c], Ilaria Palchetti [b,**], Federico Polo [a,c,*]

[a] Department of Molecular Sciences and Nanosystems, Ca' Foscari University of Venice, Via Torino 155, 30172, Venice, Italy
[b] Department of Chemistry "Ugo Schiff", University of Florence, Via della Lastruccia 3, 50019 Sesto Fiorentino (FI), Italy
[c] European Centre for Living Technology (ECLT), Ca' Bottacin, Dorsoduro 3911, Calle Crosera, Venice, 30124, Italy

ARTICLE INFO

Keywords:
Biosensor
Synthetic bioreceptors
Peptides
Urokinase-type plasminogen activator
uPA
Biomarker
Screen-printed electrodes

ABSTRACT

The use of synthetic bioreceptors to develop biosensing platforms has been recently gaining momentum. This case study compares the performance of a biosensing platform for the human biomarker urokinase-type plasminogen activator (h-uPA) when using two bicyclic peptides (P_1 and P_2) with different affinities for the target protein. The bioreceptors P_1 and P_2 were immobilized on magnetic microbeads and tested within a sandwich-type affinity electrochemical assay. Apart from enabling h-uPA quantification at nanomolar levels (105.8 ng/mL for P_1 and 32.5 ng/mL for P_2), this case study showed the potential of synthetic bicyclic peptides applicability and how bioreceptor affinity can influence the performance of the final sensing platform.

1. Introduction

Recent advances in the *in vitro* and *in silico* screening methods for the selection of biomolecules against specific targets and the characterisation of the biomolecule/target complexes allow designing a wide variety of high-affinity bioreceptors, such as aptamers, peptides, nanobodies, peptide nucleic acids (Daems et al., 2021; Liu et al., 2018; Xu et al., 2021). Despite the technological advances, selection processes are still one of the main demanding challenges in the development of biosensing platforms. These processes can be reiterated several times, starting from different libraries and using various methodologies, with the risk of getting framed in a "*never-ending*" quest for the best possible bio-recognition element. To avoid this loop, we need to develop studies and methodologies able to answer the following questions: to what extent should we improve the bioreceptor affinity? how do these improvements modify the biosensor response in terms of sensitivity/selectivity?

Peptides have been successfully applied as bioreceptors in a wide variety of biosensing platforms (mainly electrochemical, electrochemiluminescent, photoelectrochemical, and optical) to monitor metal ions, small-molecules as well as enzymes, antibodies, and even bacteria (Guida et al., 2018; Puiu and Bala, 2018). The advances in peptide selection, synthesis, and bio-conjugation/immobilization in biosensing platforms or arrays are contributing to the development of peptide-based sensors for clinical diagnostics (Xiao et al., 2018). Among these, portable electrochemical peptide-based sensors, aimed at monitoring biomarkers in biological fluids, showed promising results in terms of high selectivity and sensitivity (Campuzano et al., 2020; Wang et al., 2020). Peptide bioreceptors can fold in compact structural motifs shaping highly stable nanosized architectures and enabling a highly selective and sensitive recognition of specific analytes at subnanomolar levels, as we recently reviewed (Sfragano et al., 2021). In particular, bicyclic peptides have greater conformational rigidity and metabolic stability compared to linear and monocyclic peptides, thus enabling the recognition of challenging targets with antibody-like affinity and specificity (Karimzadeh et al., 2018; Rhodes and Pei, 2017). An in-depth understanding of the interaction mechanism between bicyclic peptides and their target molecules in the complex adduct is required prior to designing the biosensor architecture, as previously described for other bioreceptors, such as nanobodies and aptamers (Daems et al., 2021). Differences in bioreceptor affinities can deeply affect the performance of the final biosensing platform, as exemplified in this work.

Here, we investigated and compared the performance of two bicyclic peptides, as novel synthetic receptors, targeting the biomarker human urokinase-type plasminogen activator (h-uPA) (Angelini et al., 2012a). h-uPA is an extracellular protease involved in the plasminogen activator system together with the urokinase-type plasminogen activator receptor

* Corresponding author. Department of Molecular Sciences and Nanosystems, Ca' Foscari University of Venice, Via Torino 155, 30172, Venice, Italy.
** Corresponding author. Department of Chemistry "Ugo Schiff", University of Florence, Via della Lastruccia 3, 50019 Sesto Fiorentino (FI), Italy
E-mail addresses: ilaria.palchetti@unifi.it (I. Palchetti), federico.polo@unive.it (F. Polo).
[1] Co-first authors.

https://doi.org/10.1016/j.bios.2022.114477
Received 16 April 2022; Received in revised form 2 June 2022; Accepted 8 June 2022
Available online 16 June 2022

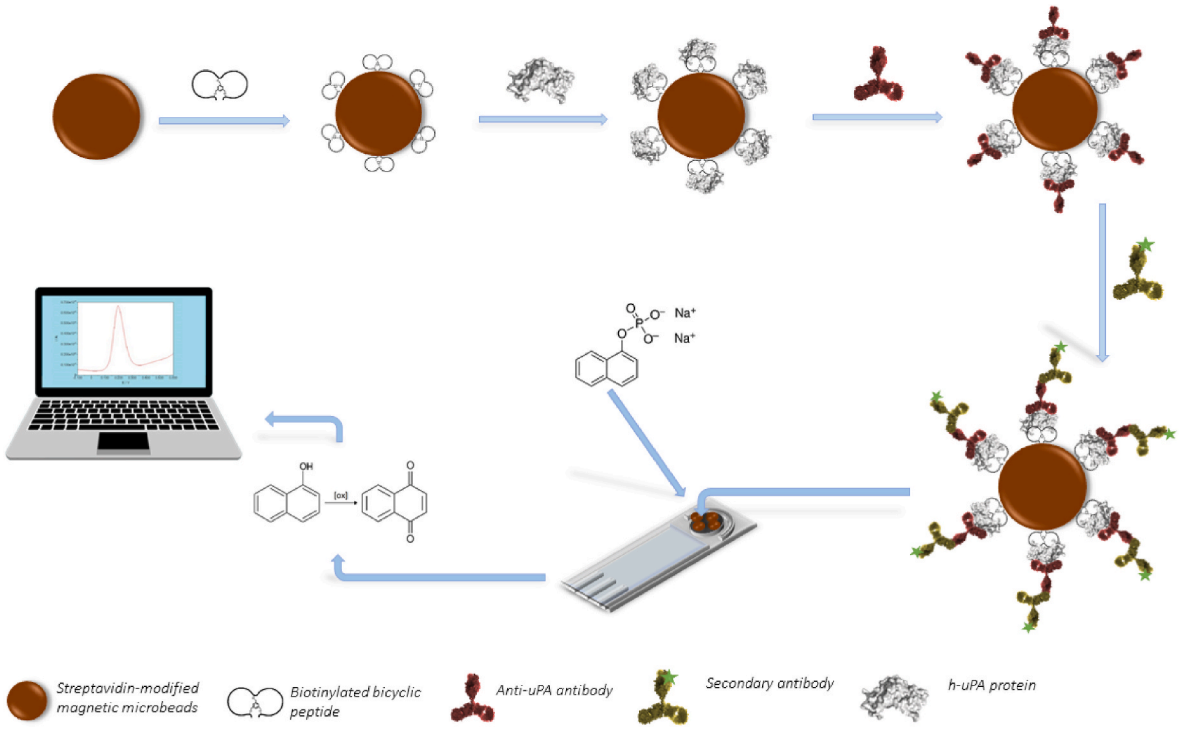

Fig. 1. Schematic of the biosensing assay. The magnetic microbeads (MB) modified with streptavidin are first functionalized with the biotinylated bicyclic peptides. Then, the MB are incubated with h-uPA spiked samples to allow the formation of the peptide-biomarker complex. Once the complex is immobilized at the MB surface, after several washing steps, the anti-uPA is added, followed by the secondary antibody (Ab_2) conjugated with alkaline phosphatase (AlkP), the labelling system. As the final step, the functionalized microbeads are immobilized on the surface of a disposable screen-printed sensor and 1-naphthyl phosphate is added in solution and converted to 1-naphthol by AlkP. The oxidation current of 1-naphthol is recorded by differential pulse voltammetry (DPV).

and plasminogen activator inhibitors 1 and 2. This system is related to various physiological and pathophysiological processes, from the degradation of extracellular matrix proteins to cancer progression and metastasis or incidence of cardiovascular diseases in haemodialysis patients (Mahmood et al., 2018; Mekkawy et al., 2014; Zhai et al., 2022). High levels of h-uPA can be associated with metastatic events and shorter survivability times. Moreover, the uPA system contributes to cardiovascular disease (CVD) in patients on haemodialysis (HD) and alteration of its functionalities might be related to COVID-19 side-effects (Chalkias et al., 2020; D'Alonzo et al., 2020; Middeldorp et al., 2020; Zanza et al., 2021).

The bicyclic peptides, namely P_1 and P_2, capable of binding the catalytic sites of h-uPA were chemically synthesized and tested as bioreceptors to develop a sandwich-type affinity electrochemical assay for h-uPA, as schematically summarized in Fig. 1. P_1 and P_2 offer two binding sites for h-uPA, and bear a biotinylated linker to allow directional and uniform immobilization on streptavidin-coated magnetic microbeads (MBs). After incubating with the h-uPA spiked samples, the peptide-functionalized MBs were incubated with a primary antibody (Ab_1), which selectively recognises complementary h-uPA sites. In a second step, they were incubated with a secondary antibody (Ab_2) conjugated with alkaline phosphatase (AlkP) serving as the labelling system. The conjugate MB-$P_{1\ or\ 2}$-[h-uPA]-Ab_1-Ab_2-AlkP complex was then magnetically immobilized at disposable screen-printed electrodes and 1-naphthyl phosphate was added in solution and converted to 1-naphthol by AlkP. The concentration of h-uPA was correlated to the current intensity of the oxidation peak of 1-naphthol, obtained by differential pulse voltammetry (DPV). The different responses of the biosensing platform employing P_1 or P_2 suggested that different kinetics are governing the recognition event. The biosensing platform, which was

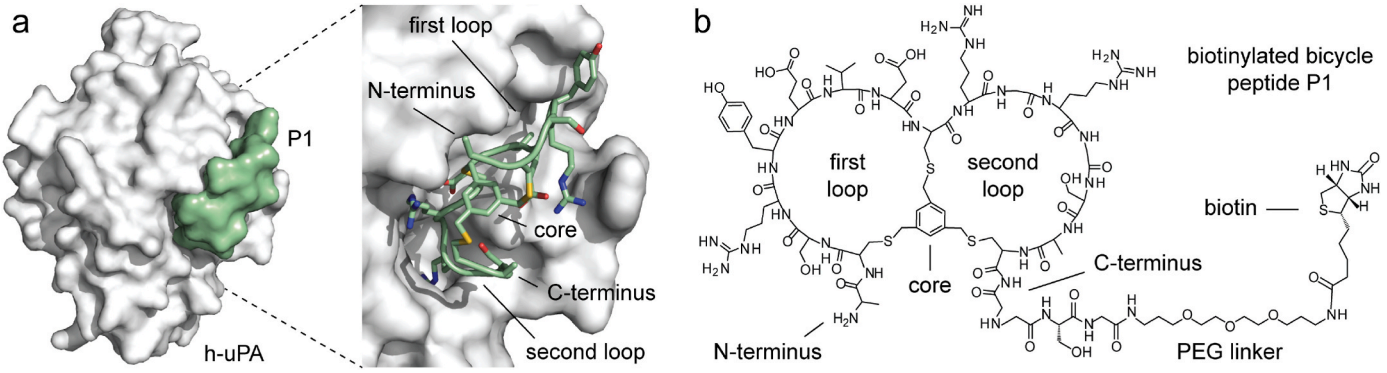

Fig. 2. (**a**) Surface representation of h-uPA (white) in complex with P_1 (light green) with a zoom-in P_1 binding site. (b) Schematic representation of the chemical structure of biotinylated bicyclic peptide P_1. Because the C-terminal end of P_1 and P_2 are freely accessible when in complex with h-uPA, as previously determined by X-ray crystallography (Angelini et al., 2012a), the biotin was linked to this end of the molecules.

tested with a portable instrumentation, showed the potential and reliability of monitoring h-uPA in serum samples.

2. Experimental section

2.1. Materials and reagents

The low-molecular-weight human urokinase plasminogen activator (LMW-h-uPA) depicted in Fig. 2a was recombinantly produced as previously reported (Angelini et al., 2012a). Diethanolamine, non-ionic surfactant polyoxyethylene-20-sorbitan monolaurate (Tween 20), streptavidin-conjugated AlkP, 1-naphthyl phosphate disodium salt, D-biotin, $Na_2HPO_4{\cdot}12H_2O$, KH_2PO_4, KCl, HCl, $MgCl_2$, NaCl, tris (hydroxymethyl)aminomethane hydrochloride (TRIS-HCl), 4-(1,1,3, 3-Tetramethylbutyl)phenyl-polyethylene glycol solution (Triton X-100), ethylenediaminetetraacetic acid (EDTA), Bovine Serum Albumin, Human Serum, Rink Amide AM resin, Fmoc-PEG Biotin resin, all amino acids required, anisole, dimethylformamide (DMF), dichloromethane (DCM), benzotriazol-1-yloxytripyrrolidinophosphonium hexafluorophosphate (PyBOP), *N*-methyl-2-pyrrolidone (NMP), triisopropylsilane (TIPS), anisole/1,8-octandithiolo, thioanisole, $(NH_4)_2CO_3$, *tert*-butyl-1,3,5-tris(bromomethyl)benzene (TBMB), piperidine, *N*-methylmorpholine (NMM), ethanol, acetic anhydride, diethyl ether, trifluoroacetic acid (TFA), methyl *tert*-butyl ether (MTBE), and the Anti-Rabbit IgG AlkP-conjugated antibody Ab_2 were purchased from Sigma-Aldrich (Merck KGaA group, Italy). NaH_2PO_4, H_2NaO_4P, acetonitrile (ACN, LC-MS grade), and formic acid were purchased from CARLOERBA (Milan, Italy). Dynabeads® MyOne™ Streptavidin C1 magnetic microparticles (MB) and the Urokinase Polyclonal Antibody Ab_1 were purchased from Invitrogen™-Thermo Fischer. The graphite screen-printed electrodes (G-SPE; DS110) were purchased from Metrohm (Italy). The ultra-pure Milli-Q water used throughout the analyses was obtained with the Millipore system (Merck) and had a resistivity of 18.2 MΩ cm. The phosphate buffer saline (PBS) at pH 7.4 was prepared by mixing 0.136 M NaCl, 2.68 mM KCl, 3.97 mM $Na_2HPO_4{\cdot}12H_2O$, and 1.46 mM KH_2PO_4. The binding and washing buffer (B&W) at pH 7.5 was obtained by mixing 10 mM Tris-HCl, 1 mM EDTA, and 2 M NaCl. The DEA buffer at pH 9.6 was made by adding 0.1 M diethanolamine, 0.1 M KCl, and 1 mM $MgCl_2$ in an aqueous solution. To each of these buffers, a 0.01% (v/v) Tween 20 was added to obtain other buffers, namely PBS + T, B&W-1x + T, and DEA + T. The B&W-1x + T was prepared by diluting the B&W-2x + T buffer (1:2 ratio).

2.2. Chemical synthesis of bicyclic peptides

Linear peptides were synthesized on the MultiPep RSi (Intavis) by standard Fmoc solid-phase peptide synthesis on a Rink Amide AM resin for the bicyclic peptides and a Fmoc-PEG Biotin resin for the biotinylated counterparts. The coupling was carried out twice for each amino acid (6 eq., 0.4 M solution in DMF) using the PyBOP/NMM coupling system (5.5 eq. 0.4M/9 eq. 4 M in DMF). Fmoc groups were removed using a 20% (v/v) solution of piperidine in DMF. The final peptide was deprotected and cleaved from the resin using a TFA/anisole/1,8-Octandithiolo/Thioanisole/H_2O mixture (90/2.5/2.5/2.5/2.5 v/v) for 3 h under shaking at room temperature. The peptide was precipitated with ice-cold diethyl ether (50 mL), then collected by centrifugation (10 min, 4000 rpm, 5 °C), washed twice with diethyl ether (20 mL) and lyophilized (LIO-5PDGT). Finally, the crude peptide (1 mM) was dissolved in 70% v/v 20 mM NH_4HCO_3, pH 8.0 and 30% v/v ACN and reacted with TBMB (1.5 mM) for 1 h at 30 °C (Angelini et al., 2012b). The crude reaction was purified by a preparative reversed-phase high-performance liquid chromatography (RP-HPLC) on a C18 column (19 × 150 mm) to obtain the final bicyclic peptides, P_1 and P_2 (Fig. 2b). The mobile phase was performed with a linear gradient of solvent B (99.9% v/v ACN, 0.1% v/v TFA) in solvent A (99.9% v/v H_2O, 0.1% v/v TFA) from 10 to 90% in 35 min. The collected fractions were freeze-dried and the molecular mass of each peptide was determined by electrospray ionisation mass spectrometry (ESI–MS) performed on a single quadrupole liquid chromatograph InfinityLab LC/MSD mass spectrometer (Agilent Technologies) coupled to a 1260 Infinity II LC system (Agilen Technologies t). The reversed-phase HPLC column was a Nucleosil 100-5 C18 (5 μm, 125 mm × 4 mm; Macherey-Nagel). The system operated with the standard ESI source and in the positive ionisation mode. For mass spectrometric analysis, the samples were mixed with 50% v/v ACN, 50% v/v H_2O. Peptides were run at a flow rate of 1 mL/min with a linear gradient of solvent B over 15 min (solvent A: 99.9% v/v H_2O and 0.1% v/v formic acid; solvent B: 99.9% v/v ACN and 0.1% v/v formic acid). Data were acquired, processed and analysed using the Agilent OpenLAB CDS (Agilent Technologies) and MestReNova (Mestrelab Research). MS analysis for P_1 (MW: 2574.1 g/mol): calculated $[M+2H]^{2+}$ = 1288.1, observed $[M+2H]^{2+}$ = 1288.5; calculated $[M+3H]^{3+}$ = 859.0, observed $[M+3H]^{3+}$ = 859.4; calculated $[M+4H]^{4+}$ = 644.5, observed $[M+4H]^{4+}$ = 644.8. MS analysis for P_2 (MW: 2553.98 g/mol): calculated $[M+2H]^{2+}$ = 1277.9, observed $[M+2H]^{2+}$ = 1277.6; calculated $[M+3H]^{3+}$ = 852.3, observed $[M+3H]^{3+}$ = 852.1; calculated $[M+4H]^{4+}$ = 639.5, observed $[M+4H]^{4+}$ = 639.4. The sequence and the structure of P_2 cannot be disclosed at the moment as it is patent-pending.

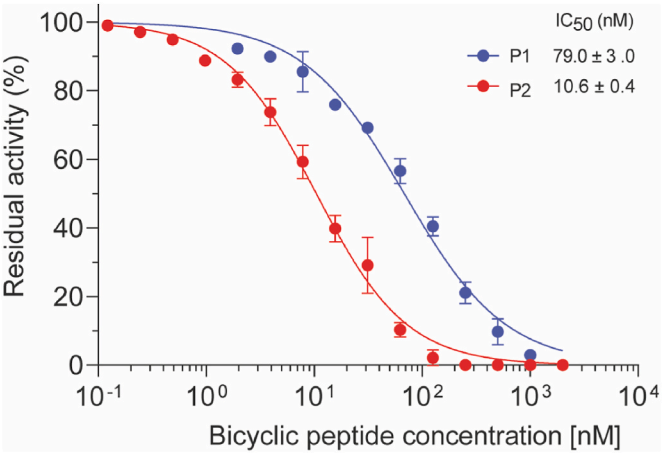

Fig. 3. Comparison of the residual activities of human h-uPA incubated with different concentrations of P_1 (blue) and P_2 (red). The average value of at least three measurements is reported as mean ± s.d. (bars). In the inset, the values of IC_{50} are provided.

2.3. Determination of inhibitory activity and specificity of bicyclic peptides

The inhibitory activity of P_1 and P_2 bicyclic peptides was assessed by monitoring the residual activity of h-uPA in the presence of different concentrations of an inhibitor and a fluorogenic substrate (Z-Gly-Gly-Arg-AMC, Bachem), as shown in Fig. 3. Residual activity is quantified by monitoring the release of fluorescent 7-amino-4-methylcoumarin (AMC) which excites at 360–380 nm and emits at 440–460 nm. The peptide inhibitory activity was measured incubating 15 nM h-uPA with 50 μM fluorogenic substrate and two-fold peptide dilutions (0 nM, 0.12 nM, 0.24 nM, 0.48 nM, 0.97 nM, 1.95 nM, 3.9 nM, 7.81 nM, 15.6 nM, 31.2 nM, 62.5 nM, 125 nM, 250 nM, 500 nM, 1000 nM, 2000 nM). All reagents were previously diluted in Buffer R* (10 mM TRIS-HCl, pH 7.4, 150 mM NaCl, 10 mM $MgCl_2$, 1 mM $CaCl_2$, 1% w/v BSA, and 0.1% v/v Triton-X100). Measurements were performed on a Tecan microplate reader at room temperature, for 30 min, under shaking with an excitation wavelength of 355 nm and an emission recording at 460 nm (Angelini et al., 2012a).

2.4. Preparation of bioreceptor-functionalized magnetic beads

The biotinylated peptides P_1 and P_2 were immobilized at streptavidin-coated magnetic beads (MBs). The commercially available MBs used in this work have an expected diameter of 1 μm, as specified in the manufacturer's technical sheet, and have already been used for the development of an electrochemical assay for nucleic acid and protein detection (Baydemir et al., 2016). 25 μL of MBs were pipetted into a 1.5 mL vial, followed by three washing steps with B&W-2x, B&W-1x + T and PBS + T, respectively, using a magnetic rack to collect and isolate them from the buffer. 200 μL PBS containing 1 μL of 2 mg/mL biotinylated bicyclic peptide (770 pmol) were added to the suspension of the MBs. After 30 min of incubation under continuous mixing, the MBs were washed twice with PBS + T. To block the potentially remaining active sites of streptavidin, the modified-MBs were incubated with a 1 mM biotin solution in PBS. Finally, after a washing step with PBS + T, the MBs were re-suspended in 200 μL of PBS + T and stored at +4 °C.

2.5. Analytical protocol for sandwich-type affinity electrochemical assay for h-uPA

The bicyclic peptide-modified MBs described above were washed once with PBS and then incubated for 20 min with h-uPA spiked samples in PBS, under continuous mixing. Two washing steps with PBS + T and one with PBS followed. 2 μg/mL of Ab_1 in PBS were incubated with the modified MBs for 15 min. After two subsequent washing steps with DEA + T and one with DEA, the beads were incubated again for 15 min with a 2 μg/mL solution of Ab_2 in DEA. 2 final washing steps with DEA + T and 2 with DEA completed the procedure, and the beads were resuspended in 50 μL of DEA. 10 μL of the resuspended modified-MBs were magnetically immobilized at disposable screen-printed carbon electrodes and incubated for 5 min with a 0.5 mg/mL 1-naphthyl phosphate solution in DEA. Overall, the assay as described above can be performed in 1 h. Then, DPV measurements can be carried out, and only a couple of minutes are required to record the electrochemical readout.

3. Results and discussion

3.1. Comparison of P_1 and P_2 binding affinity

The performances of the biosensing platform were tested by employing two bicyclic peptides, namely P_1 and P_2. These synthetic receptors are capable of selectively binding the active site of h-uPA, thus enabling a specific recognition of its active form (Angelini et al., 2012a). The inhibitory activity of P_1 and P_2 was assessed by monitoring the residual activity of h-uPA with different concentrations of inhibitor and in the presence of a fluorogenic substrate, as shown in Fig. 3. The determined IC_{50} values (79 ± 3 for P_1 and 10.6 ± 0.4 for P_2) were then used to obtain the inhibitory activity constant (K_i) of both bioreceptors. P_1 showed a K_i of 55 ± 8 nM, whereas P_2 revealed a K_i of 7.4 ± 0.9 nM. The amino acid sequences of P_1 and P_2 vary by solely four residues (Fig. 2), but even such a small variation in the sequence can deeply influence the affinity of the peptide toward their target accounting for the ~7-fold difference observed in the K_i values. The values of K_i are related to the binding affinity: the smaller the K_i, the greater the binding affinity towards its ligand. Although both showed good inhibitory activity, the IC_{50} values imply that the concentration of P_2 needed to inhibit an equal concentration of h-uPA is less than half the concentration required when using P_1. Therefore, these results show that: *i)* even though the amino acid sequences are quite similar, their binding affinity for h-uPA is significantly different; *ii)* P_2 has a greater affinity for h-uPA compared to P_1. The preliminary IC_{50} characterisation led us investigating the possibility to test and compare the two sequences, although their affinity towards the target protein differs within a relatively narrow range.

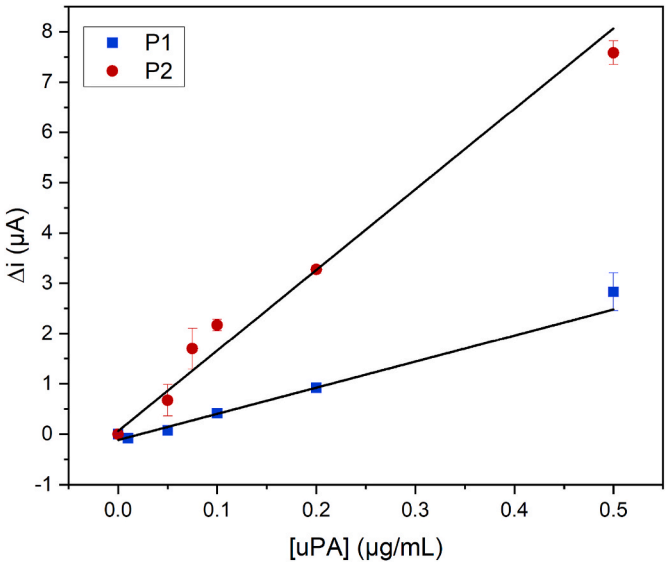

Fig. 4. Calibration plots of P1 (blue squares) and P2 (red dots) compared in the same linear region 0.0–0.5 μg/mL.

3.2. P_1 and P_2 performances in the biosensing platform

Both biotinylated P1 and P2 were integrated as biorecognition elements in the biosensing platform by employing the same experimental conditions, which allowed comparing the two datasets obtained and evaluating whether the biosensing platform would give a different response in the presence of slightly different amino acid sequences. All measurements were performed in triplicate, as described in Section 2.5. In particular, the calibration plots were obtained by measuring the oxidation current of 1-naphthol produced enzymatically by means of DPV. In Fig. 4, the Δi represents the difference between the oxidation current of 1-naphthol measured at a specific h-uPA concentration and the corresponding current measured in the blank sample. The two calibration plots were interpolated by linear regression in the range from 0.0 μg/mL to 0.5 μg/mL. The comparison between the linear trends obtained with both bicyclic peptides makes the difference in the performance of the two biosensing platforms evident. The slope of the plot relative to P_2 was found to be 16.0 ± 0.9, which was three times higher than that of P_1 (of about 5.2 ± 0.3). This evidence suggests distinct sensitivities of the two platforms. The LODs were estimated considering the average response of the blank plus 3-times its standard deviation, thus providing 105.8 ng/mL and 32.5 ng/mL for P_1 and P_2, respectively. Such a discrepancy can be ascribed to the different affinity of the two bioreceptors for h-uPA. In other terms, two similar bicyclic peptides with only a few differences in the amino acid sequence can exhibit a meaningfully different response in the overall outcome of the analytical assay.

3.3. Assessing the matrix effect

The main advantage when using magnetic beads lies in the ease of extraction procedure of the analyte that significantly reduces the matrix effect (ME). Once the analyte is captured onto the beads, it is magnetically removed from the matrix and the remaining steps of the assay can be carried out in buffer solution. As a proof-of-concept, ME was evaluated by comparing the signals obtained in buffer solution with those obtained in 10-fold diluted human serum spiked with h-uPA in the concentration range 0–10 μg/mL, thus covering three orders of magnitude. In particular, the ME% was calculated by multiplying 100 times the ratio between the signal of 1-naphthol obtained in spiked serum and the corresponding signal obtained in buffer solution (Caban et al., 2012; Matuszewski et al., 1998). The closer this value is to 100%, the lesser the

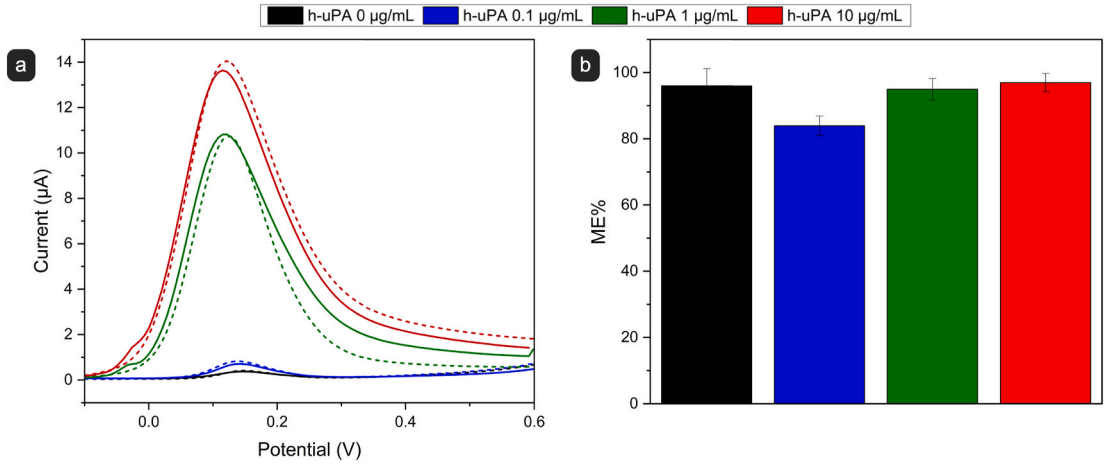

Fig. 5. (**a**) DPV recorded in buffer (dashed line —) and diluted serum (solid line —) at different h-uPA concentrations (**b**) Matrix effect expressed in percentage (ME %) per each h-uPA concentration tested.

matrix influences the analysis. The 96% value in ME% obtained for the blank sample, in absence of h-uPA, suggests an almost identical behaviour of the platform against nonspecific binding in buffer solution and diluted serum (Fig. 5 a-b). In the presence of h-uPA, a ME% > 80% was found in the investigated concentration range. Therefore, it can be assumed that, although the matrix appears to affect the performance of the platform, its influence is significantly reduced.

4. Conclusions

In this case study, the development of a biosensing platform to detect the cancer biomarker h-uPA by employing synthetic receptors, based on selected bicyclic peptide sequences, coupled with antibodies is described. A magnetic beads-based sandwich assay combined with an electrochemical readout was tested using two bicyclic peptides, P_1 and P_2, whose sequences differ only by 4 amino acids. A ~7-fold difference in the K_i values was found for P_2 compared to P_1 and ascribed to the variation in the amino acid chain. Calibration plots were obtained with both peptides, showing that the difference in the binding affinity results in a deep change in the biosensor performances in terms of sensitivity, particularly for low h-uPA concentrations (<0.1 μg/mL). The applicability of this sensing platform was further tested in diluted serum samples observing a limited matrix effect with ME% > 80% in the concentration range investigated. This case study highlights that the affinity constant towards the target might lead to major discrepancies in the overall reliability of the biosensing platform. Therefore, it is extremely important to test and compare different peptide sequences and correlate their affinities with their performance as bioreceptor once integrated in the biosensor architecture. The results of this study also suggest that: *i)* when a biosensing platform showed poor performance (especially in terms of sensitivity), one should consider investing in the improvement of the bioreceptor selection; *ii)* if the biosensor can detect the target in the concentration range of interest with a good sensitivity/selectivity/reproducibility, there is no need to reiterate the selection process. Compromising between the selection of high-affinity bioreceptors and the design of a biosensing platform able to answer specific analytical queries is instrumental to the rapid development of point-of-care diagnostics. In particular, bicyclic peptide-based sensing strategies seem to be very promising thanks to their stability, limited production costs and high performance. Eventually, we would also like to stress the importance of synthetic receptors in the development of biosensing platforms, as their use is recently gaining momentum. The selected bicyclic peptides employed in this work are an example of what next-generation biosensing platforms might look like, regardless the fact whether a labelling system is also employed or not (e.g. optical-based technology, such as surface plasmon resonance, SPR, technology does not need it). In fact, the use of synthetic receptors, other than aptamers, might help limiting or (in the best-case scenario) avoiding the use of the "natural" ones, which might not be commercially available for a specific target and/or, when they are, they might be expensive, difficult to obtain and purify in high amount.

Author contributions statement

Giulia Moro and Patrick Severin Sfragano: performed the experimental measurements, analysed the whole set of data, actively contributed in drafting and revising the manuscript. Jessica Ghirardo: synthesized the peptides and actively contributed in performing the experimental measurements. Ylenia Mazzocato: characterized the peptides and performed the IC_{50} measurements, and actively contributed in analyzing the data pertaining the inhibition kinetics. Alessandro Angelini: supervised the synthesis and characterization of the peptides and actively contributed in revising the manuscript. Ilaria Palchetti and Federico Polo: conceived the project, supervised the entire research activity, wrote the draft, finalize and revised the manuscript. All authors interpreted the results and discussed extensively. All authors reviewed and approved the final version of the manuscript.

Declaration of competing interest

The authors declare that they have no known competing financial interests or personal relationships that could have appeared to influence the work reported in this paper.

References

Angelini, A., Cendron, L., Chen, S., Touati, J., Winter, G., Zanotti, G., Heinis, C., 2012a. Bicyclic peptide inhibitor reveals large contact interface with a protease target. ACS Chem. Biol. 7, 817–821. https://doi.org/10.1021/cb200478t.

Angelini, A., Morales-Sanfrutos, J., Diderich, P., Chen, S., Heinis, C., 2012b. Bicyclization and tethering to Albumin yields long-acting peptide antagonists. J. Med. Chem. 55, 10187–10197. https://doi.org/10.1021/jm301276e.

Baydemir, G., Bettazzi, F., Palchetti, I., Voccia, D., 2016. Strategies for the development of an electrochemical bioassay for TNF-alpha detection by using a non-immunoglobulin bioreceptor. Talanta 151, 141–147. https://doi.org/10.1016/j.talanta.2016.01.021.

Caban, M., Migowska, N., Stepnowski, P., Kwiatkowski, M., Kumirska, J., 2012. Matrix effects and recovery calculations in analyses of pharmaceuticals based on the determination of β-blockers and β-agonists in environmental samples. J. Chromatogr. A 1258, 117–127. https://doi.org/10.1016/j.chroma.2012.08.029.

Campuzano, S., Pedrero, M., Gamella, M., Serafín, V., Yáñez-Sedeño, P., Pingarrón, J.M., 2020. Beyond sensitive and selective electrochemical biosensors: towards continuous, real-time, antibiofouling and calibration-free devices. Sensors. https://doi.org/10.3390/s20123376.

Chalkias, A., Mouzarou, A., Samara, E., Xanthos, T., Ischaki, E., Pantazopoulos, I., 2020. Soluble urokinase plasminogen activator receptor: a biomarker for predicting complications and critical care admission of COVID-19 patients. Mol. Diagnosis Ther. 24, 517–521. https://doi.org/10.1007/s40291-020-00481-8.

D'Alonzo, D., De Fenza, M., Pavone, V., 2020. COVID-19 and pneumonia: a role for the uPA/uPAR system. Drug Discov. Today 25, 1528–1534. https://doi.org/10.1016/j.drudis.2020.06.013.

Daems, E., Moro, G., Campos, R., De Wael, K., 2021. Mapping the gaps in chemical analysis for the characterisation of aptamer-target interactions. TrAC Trends Anal. Chem. 142, 116311 https://doi.org/10.1016/j.trac.2021.116311.

Guida, F., Battisti, A., Gladich, I., Buzzo, M., Marangon, E., Giodini, L., Toffoli, G., Laio, A., Berti, F., 2018. Peptide biosensors for anticancer drugs: design in silico to work in denaturizing environment. Biosens. Bioelectron. 100, 298–303. https://doi.org/10.1016/j.bios.2017.09.012.

Karimzadeh, A., Hasanzadeh, M., Shadjou, N., Guardia, M. de la, 2018. Peptide based biosensors. TrAC Trends Anal. Chem. 107, 1–20. https://doi.org/10.1016/j.trac.2018.07.018.

Liu, W., Song, H., Chen, Q., Yu, J., Xian, M., Nian, R., Feng, D., 2018. Recent advances in the selection and identification of antigen-specific nanobodies. Mol. Immunol. 96, 37–47. https://doi.org/10.1016/j.molimm.2018.02.012.

Mahmood, N., Mihalcioiu, C., Rabbani, S.A., 2018. Multifaceted role of the urokinase-type plasminogen activator (uPA) and its receptor (uPAR): diagnostic, prognostic, and therapeutic applications. Front. Oncol. 8 https://doi.org/10.3389/fonc.2018.00024.

Matuszewski, B.K., Constanzer, M.L., Chavez-Eng, C.M., 1998. Matrix effect in quantitative LC/MS/MS analyses of biological fluids: a method for determination of finasteride in human plasma at picogram per milliliter concentrations. Anal. Chem. 70, 882–889. https://doi.org/10.1021/ac971078+.

Mekkawy, A.H., Pourgholami, M.H., Morris, D.L., 2014. Involvement of urokinase-type plasminogen activator system in cancer: an overview. Med. Res. Rev. 34, 918–956. https://doi.org/10.1002/med.21308.

Middeldorp, S., Coppens, M., van Haaps, T.F., Foppen, M., Vlaar, A.P., Müller, M.C.A., Bouman, C.C.S., Beenen, L.F.M., Kootte, R.S., Heijmans, J., Smits, L.P., Bonta, P.I., van Es, N., 2020. Incidence of venous thromboembolism in hospitalized patients with COVID-19. J. Thromb. Haemost. 18, 1995–2002. https://doi.org/10.1111/jth.14888.

Puiu, M., Bala, C., 2018. Peptide-based biosensors: from self-assembled interfaces to molecular probes in electrochemical assays. Bioelectrochemistry 120, 66–75. https://doi.org/10.1016/j.bioelechem.2017.11.009.

Rhodes, C.A., Pei, D., 2017. Bicyclic peptides as next-generation therapeutics. Chem. – A Eur. J. 23, 12690–12703. https://doi.org/10.1002/chem.201702117.

Sfragano, P.S., Moro, G., Polo, F., Palchetti, I., 2021. The role of peptides in the design of electrochemical biosensors for clinical diagnostics. Biosens. https://doi.org/10.3390/bios11080246.

Wang, G., Han, R., Li, Q., Han, Y., Luo, X., 2020. Electrochemical biosensors capable of detecting biomarkers in human serum with unique long-term antifouling abilities based on designed multifunctional peptides. Anal. Chem. 92, 7186–7193. https://doi.org/10.1021/acs.analchem.0c00738.

Xiao, X., Kuang, Z., Slocik, J.M., Tadepalli, S., Brothers, M., Kim, S., Mirau, P.A., Butkus, C., Farmer, B.L., Singamaneni, S., Hall, C.K., Naik, R.R., 2018. Advancing peptide-based biorecognition elements for biosensors using in-silico evolution. ACS Sensors 3, 1024–1031. https://doi.org/10.1021/acssensors.8b00159.

Xu, P., Ghosh, S., Gul, A.R., Bhamore, J.R., Park, J.P., Park, T.J., 2021. Screening of specific binding peptides using phage-display techniques and their biosensing applications. TrAC Trends Anal. Chem. 137, 116229. https://doi.org/10.1016/j.trac.2021.116229.

Zanza, C., Racca, F., Longhitano, Y., Piccioni, A., Franceschi, F., Artico, M., Abenavoli, L., Maiese, A., Passaro, G., Volonnino, G., Russa, R. La, 2021. Risk management and treatment of coagulation disorders related to COVID-19 infection. Int. J. Environ. Res. Public Health 18, 1–16. https://doi.org/10.3390/ijerph18031268.

Zhai, B.-T., Tian, H., Sun, J., Zou, J.-B., Zhang, X.-F., Cheng, J.-X., Shi, Y.-J., Fan, Y., Guo, D.-Y., 2022. Urokinase-type plasminogen activator receptor (uPAR) as a therapeutic target in cancer. J. Transl. Med. 20, 135. https://doi.org/10.1186/s12967-022-03329-3.